A Structural Mode-Coupling Approach to ^{15}N NMR Relaxation in Proteins

Vitali Tugarinov,[‡] Zhichun Liang,[§] Yury E. Shapiro,[‡] Jack H. Freed,*[,§] and Eva Meirovitch*[,‡]

Contribution from the Faculty of Life Sciences, Bar-Ilan University, Ramat-Gan 52900, Israel, and Baker Laboratory of Chemistry and Chemical Biology, Cornell University, Ithaca, New York 14853-1301

Received October 30, 2000. Revised Manuscript Received January 8, 2001

Abstract: The two-body Slowly Relaxing Local Structure (SRLS) model was applied to ^{15}N NMR spin relaxation in proteins and compared with the commonly used original and extended model-free (MF) approaches. In MF, the dynamic modes are assumed to be decoupled, local ordering at the N−H sites is represented by generalized order parameters, and internal motions are described by effective correlation times. SRLS accounts for dynamical coupling between the global diffusion of the protein and the internal motion of the N−H bond vector. The local ordering associated with the coupling potential and the internal N−H diffusion are tensors with orientations that may be tilted relative to the global diffusion and magnetic frames. SRLS generates spectral density functions that differ from the MF formulas. The MF spectral densities can be regarded as limiting cases of the SRLS spectral density. SRLS-based model-fitting and model-selection schemes similar to the currently used MF-based ones were devised, and a correspondence between analogous SRLS and model-free parameters was established. It was found that experimental NMR data are sensitive to the presence of mixed modes. Our results showed that MF can significantly overestimate order parameters and underestimate local motion correlation times in proteins. The extent of these digressions in the derived microdynamic parameters is estimated in the various parameter ranges, and correlated with the time scale separation between local and global motions. The SRLS-based analysis was tested extensively on ^{15}N relaxation data from several isotropically tumbling proteins. The results of SRLS-based fitting are illustrated with RNase H from *E. coli*, a protein extensively studied previously with MF.

Introduction

The ability to interpret nuclear spin relaxation properties in terms of microdynamic parameters turned NMR into a powerful method for elucidating protein dynamics.[1,2] The amide ^{15}N spin in proteins is a particularly useful probe, relaxed predominantly by dipolar coupling to the amide proton and ^{15}N chemical shift anisotropy (CSA).[3] The experimental NMR observables (^{15}N T_1, T_2, and ^{15}N−{^{1}H} NOE acquired at one or more magnetic fields) are controlled by the global and local dynamic processes experienced by the N−H bond vector. The model-free (MF) approach in its original[4,5] and extended[6] forms is currently the most popular means of analyzing experimental NMR data in terms of microdynamic parameters associated with the N−H bond vector motions. One of the fundamental assumptions underlying the MF formulation is that the global diffusion of the protein and the internal motion of the N−H bond vector are not correlated (coupled). This "decoupling" approximation allows one to separate the two types of motions and represents the autocorrelation function, $C(t)$, of the overall dynamic process as a product of the global, $C_o(t)$, and the internal, $C_i(t)$, correlation functions:[4,5]

$$C(t) = C_o(t)\, C_i(t) \tag{1}$$

The resulting spectral density function, $J(\omega)$, is given by a weighted sum of Lorentzians. This assumption is preserved in the extended MF treatment[6] although the resulting time scale separation between the global diffusion and the slow local (nanosecond) motion is typically only about 1 order of magnitude.

Recently, a semiempirical mode-coupling diffusion approach was developed[7,8] and applied to the derivation of local dynamics in proteins.[9] However, experimental ^{15}N T_1 patterns could not be reproduced for magnetic fields exceeding 8.4 T, where the contribution of local motions becomes significant. This approach is based on molecular dynamics simulations and cannot reliably account for slower motions in proteins.[9] The common MF approach also has been extended by applying the Gaussian Axial Fluctuations (GAF) model,[10−12] which interprets the generalized

* Address correspondence to these authors. E.M.: E-mail: eva@nmrsgi1.ls.biu.ac.il. Phone 972-3-5318049. Fax: 972-3-5351824. J.H.F.: E-mail: jhf@msc.cornell.edu. Phone: 607-255-3647. Fax: 607-255-0595.

‡ Bar-Ilan University.

§ Cornell University.

(1) Kay, L. E. *Nat. Struct. Biol. NMR Suppl.* **1998**, *5*, 513−516.
(2) Ishima, R.; Torchia, D. A. *Nat. Struct. Biol.* **2000**, *7*, 740−743.
(3) Peng, J. W.; Wagner, G. *Methods Enzymol.* **1994**, *239*, 563−595.
(4) Lipari, G.; Szabo, A. *J. Am. Chem. Soc.* **1982**, *104*, 4546−4559.
(5) Lipari, G.; Szabo, A. *J. Am. Chem. Soc.* **1982**, *104*, 4559−4570.
(6) Clore, G. M.; Szabo, A.; Bax, A.; Kay, L. E.; Driscoll, P. C.; Gronenborn, A. M. *J. Am. Chem. Soc.* **1990**, *112*, 4989−4991.
(7) La Penna, G.; Pratolongo, R.; Perico, A. *Macromolecules* **1999**, *32*, 506−513.
(8) Fausti, S.; La Penna, G.; Cuniberti, C.; Perico, A. *Biopolymers* **1999**, *50*, 613−629.
(9) La Penna, G.; Fausti, S.; Perico, A.; Ferretti, J. A. *Biopolymers* **2000**, *54*, 89−103.
(10) Brüschweiler, R; Wright, P. E. *J. Am. Chem. Soc.* **1994**, *116*, 8426−8427.
(11) Bremi, T.; Brüschweiler, R. *J. Am. Chem. Soc.* **1997**, *119*, 6672−6673.

10.1021/ja003803v CCC: $20.00
Published on Web 03/08/2001

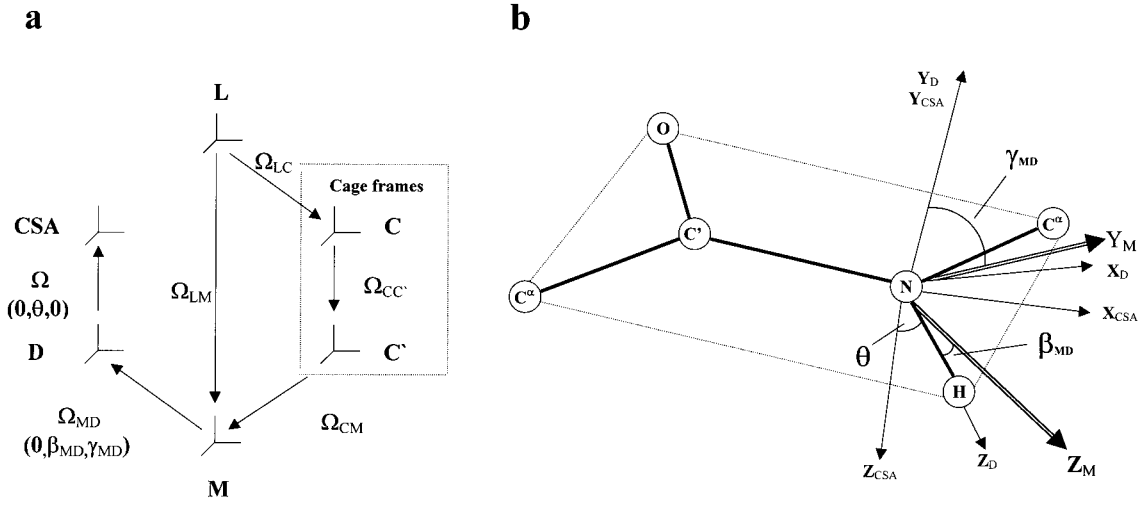

Figure 1. (a) Schematic representation of the coordinate frames used in the calculation of the SRLS spectral density function for the N−H bond vector motions: L, the laboratory frame; C, the global diffusion frame; C′, the local ordering (or local director) frame; M, the local (internal) diffusion frame; D, the dipolar ^{15}N−^{1}H tensor frame; and CSA, the ^{15}N CSA tensor frame. In the case of isotropic global tumbling the C and C′ frames become the same (cage frame). (b) Definition of the Euler angles associated with the relative orientation of the ^{15}N CSA tensor (X_{CSA}, Y_{CSA}, Z_{CSA}) and dipolar ^{15}N−^{1}H tensor (X_D, Y_D, Z_D) frames. Y_M and Z_M are principal axes of the collinear internal diffusion and local ordering tensors. The principal axes X_{CSA}, Y_{CSA}, and Z_{CSA} are defined to be aligned with the most shielded (σ_{11}), intermediate (σ_{22}), and least shielded (σ_{33}) components of the ^{15}N shielding tensor, respectively. Y_D and Y_{CSA} are assumed to be perpendicular to the peptide plane.[23] The M → D frame transformation consists of a rotation by an angle β_{MD} about Y_M and a rotation by an angle γ_{MD} about the new orientation of Z_D. The D → CSA transformation consists of a rotation by an angle θ about Y_{DD} (Y_{CSA}).

order parameter in terms of fast fluctuations about three orthogonal axes, but otherwise preserves the MF spectral density.

Here, we report on the analysis of NMR ^{15}N relaxation data using the Slowly Relaxing Local Structure (SRLS) model. SRLS was implemented originally[13,14] as an approximate theory appropriate for small local ordering and applied to ESR spin probes and NMR in liquid crystals.[14] In recent years SRLS was developed into a comprehensive rigorous structural two-body mode-coupling theory[15,16] and applied to ESR studies of biomolecular dynamics.[17−19] In the latter application the two coupled modes represent the global motion of the macromolecule and the internal motion of the spin-bearing moiety. In the context of amide ^{15}N spin relaxation in proteins, SRLS is a powerful theoretical tool that rigorously accounts for the dynamical coupling between the global diffusion of the protein and the local diffusion of the N−H bond vector. In SRLS, the global diffusion, the local diffusion, the local ordering, and the magnetic interactions are tensors that may be tilted relative to one another. The time-independent geometric relations contain important information related to protein structure. The SRLS theory can be viewed as a generalization of MF. For low ordering SRLS was shown theoretically to converge to MF in the motional narrowing limit.[15] In the present study the computational SRLS methodology[15,16] was adapted to the calculation of spectral densities for NMR spin relaxation in the case of isotropic global tumbling. The SRLS model was parametrized in a way very similar to the conventionally employed MF parametrization, and used to fit NMR experimental relaxation data. Our results show that model-free can significantly overestimate order parameters and underestimate local motion correlation times. The extent of these digressions in the derived microdynamic parameters was estimated in the various parameter ranges, and correlated with the time scale separation between the local and global motions.

Theory

The fundamentals of SRLS theory, discussed recently in the context of biomolecular dynamics,[17−19] are directly applicable to N−H bond vector motions in proteins. The coordinate frames required to describe the SRLS model are depicted in Figure 1a. The laboratory frame (L) is a space-fixed frame with its *z*-axis along the applied magnetic field. CSA and D are the ^{15}N chemical shift anisotropy and the N−H dipolar magnetic tensor frames, respectively. The dipolar tensor frame has its *z*-axis aligned along the N−H bond (Figure 1b). The Euler angles Ω_{LD} and Ω_{LCSA} are the usual stochastic variables of magnetic resonance spin relaxation, modulated by local motion of the N−H bond vector and the global molecular tumbling. The internal diffusion frame (M) relates to the local N−H bond vector motions. The M frame can be tilted relative to the N−H bond (or D frame) by a set of time-independent Euler angles $\Omega_{MD}(\alpha_{MD}, \beta_{MD}, \gamma_{MD})$. If we assume the local motion to be axially symmetric only two angles, β_{MD} and γ_{MD}, remain. The global diffusion frame (C) is a molecule-fixed frame determined mainly by the protein shape. The N−H bond vector diffuses in a highly anisotropic environment (due to geometrical and structural/motional restrictions) and experiences a mean orienting potential with symmetry axes that may be different from the C frame. We therefore define an internal ordering (director) frame (C′) that is fixed relative to the C frame. For isotropic global tumbling the distinction between C and C′ frames vanishes and they become the same (cage frame in Figure 1a, denoted as C below). To summarize, the local diffusion of the N−H bond vector and the local ordering induced by the globally tumbling surroundings (cage) are represented by tensors that

(12) Lienin, S. F.; Bremi, T.; Brütscher, B.; Brüschweiler, R.; Ernst, R. R. *J. Am. Chem. Soc.* **1998**, *120*, 9870−9879.
(13) Polnaszek, C. F.; Freed, J. H. *J. Phys. Chem.* **1975**, *79*, 2283−2292.
(14) Freed, J. H. *J. Chem. Phys.* **1977**, *66*, 4183−4199.
(15) Polimeno, A.; Freed, J. H. *Adv. Chem. Phys.* **1993**, *83*, 89−163.
(16) Polimeno, A.; Freed, J. H. *J. Phys. Chem.* **1995**, *99*, 10995−11012.
(17) Liang, Z.; Freed, J. H. *J. Phys. Chem. B* **1999**, *103*, 6384−6396.
(18) Liang, Z.; Freed, J. H.; Keyes, R.; Bobst, A. M. *J. Phys. Chem. B* **2000**, *104*, 5372−5381.
(19) Barnes, J. P.; Liang, Z.; Mchaourab, H. S.; Freed, J. H.; Hubbell, W. L. *Biophys. J.* **1999**, *76*, 3298−3306.

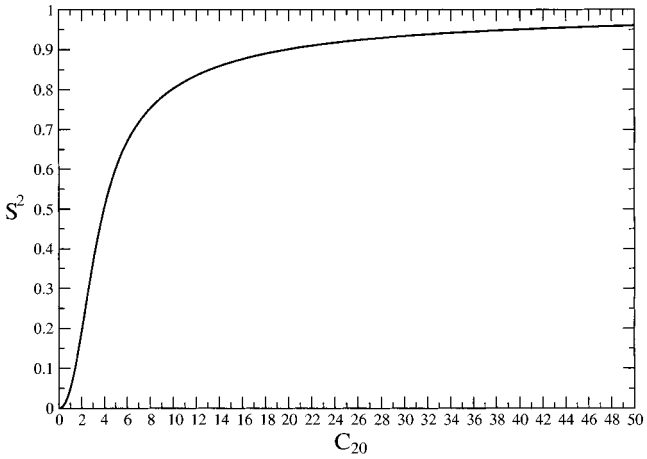

Figure 2. A plot of the square of the order parameter (S^2) versus the potential coefficient c_{20} given in units of k_BT.

may be tilted relative to the N−H bond vector (D frame) and the CSA tensor.

The N−H bond vector motions and the cage are dynamically coupled by a potential $U(\Omega_{CM})$ that depends on their relative orientation through time-dependent Euler angles $\Omega_{CM}(t)$. The coupling potential tends to align the N−H bond vector toward the *z*-axis of the ordering frame. In the simplest case of axially symmetric local ordering it is given by:[17−19]

$$U(\Omega_{CM})/k_BT = -c_{20}D^2_{00}(\Omega_{CM}) \equiv -u(\Omega_{CM}) \qquad (2)$$

where k_B is the Boltzmann constant, T the temperature in K, c_{20} the potential strength in units of k_BT, and D^2_{00} the Wigner rotation matrix element. A conventional order parameter can be related to c_{20} as:[17]

$$S = \langle D^2_{00}[\Omega_{CM}(t)]\rangle \qquad (3)$$

where

$$\langle D^2_{00}[\Omega_{CM}(t)]\rangle = \int D^2_{00}(\Omega)\exp[c_{20}D^2_{00}(\Omega)]\,d\Omega / \int \exp[c_{20}D^2_{00}(\Omega)]\,d\Omega.$$

A plot of the squared order parameter, S^2, versus c_{20} is shown in Figure 2. It should be noted that the very definition of S requires axial (or lower) symmetry of the internal diffusion tensor.[4,17]

The time-dependent part of the spin Hamiltonian for this two-body system is given by:[17]

$$\hat{H} = \sum_{\mu=CSA,\,D}\sum_{l=0,2}\sum_{m=-1}^{l}\sum_{m'=-1}^{l}\sum_{m''=-1}^{l}\hat{A}^{(l,m)}_{\mu,L}D^{l}_{mm'}(\Omega_{LM})\,D^{l}_{m'm''}(\Omega_{MCSA})F^{(l,m'')}_{\mu,CSA}* \qquad (4)$$

where $X^{(l,m)}_{\mu,N}$ stands for the mth component of the lth ($l = 0, 2$) rank irreducible spherical tensor or tensor operator X (where X is either a spin operator $\hat{A}$ or a magnetic tensor F) defined in the N frame, with μ specifying the kind of interaction (^{15}N CSA or ^{15}N−^{1}H dipolar). $D^{l}_{nm'}(\Omega_{N,N'})$ are Wigner rotation matrix elements which relate the N frame to the N′ frame. The detailed form of $\hat{A}^{(l,m)}_{\mu,L}$ and $F^{(l,m'')}_{\mu,CSA}$ can be found elsewhere.[20]

(20) Freed, J. H. *Spin labeling: Theory and Applications*; Berliner L. J., Ed.; Academic Press: New York, 1976; p 53.

The dynamic effects of the global and the local diffusion are incorporated into the spectral density through the diffusion operator:[16,17]

$$\hat{\Gamma} = \hat{\Gamma}^{global}(\Omega_{LC}) + \hat{\Gamma}^{local}(\Omega_{LM}) + F^{global}(-\Omega_{CM}) + F^{local}(\Omega_{CM}) \qquad (5)$$

The first two terms in this equation refer to freely diffusing global motion and local motion rotors. In this study the global diffusion is assumed to be isotropic (C ≡ C′; Figure 1a). Hence, $\hat{\Gamma}^{global}(\Omega_{LC})$ is given by:

$$\hat{\Gamma}^{global}(\Omega_{LC}) + R^C\,\hat{J}^{C2} \qquad (6)$$

where $\hat{J}^C$ is the infinitesimal rotation operator associated with this motion (and the super 2 implies the square), and $R^C = 1/(6\tau_m)$ is the diffusion constant for the global motion. The internal motion is given by an axially symmetric diffusion tensor:

$$\hat{\Gamma}^{local}(\Omega_{LM}) = R_\perp\,\hat{J}^{L2} + (R_{||} - R_\perp)\hat{J}^{L2}_z \qquad (7)$$

where $\hat{J}^L$ is the infinitesimal rotation operator for the local motion with the z component, $\hat{J}^L_z$, and $R_\perp$ and $R_{||}$ are the principal values of the axial local diffusion tensor. The local motion within the macromolecule (cage) is restricted by the internal orienting potential $U(\Omega_{CM})$ (eq 2), which couples the global and local motions. The last two terms in eq 5 reflect the contributions to $\hat{\Gamma}$ due to $U(\Omega_{CM})$. F^{global} and F^{local} are functions of the Euler angles Ω_{CM} that transform the M frame into the C frame, which can be further expressed as $(-\Omega_{LC} + \Omega_{LM})$ (Figure 1a). The operator expressions for F^{global} and F^{local} are given by:[17]

$$F^{local} = (1/2)[R^L_\perp(\hat{J}^{L2}\,u) + (R^L_{||} - R^L_\perp)(\hat{J}^{L2}_z\,u)] - 1/4[R^L_\perp(\hat{J}^L_+\,u)(\hat{J}^L_-\,u) + R^L_{||}\,(\hat{J}^L_z\,u)^2] \qquad (8)$$

and

$$F^{global} = (1/4)R^C[(2\hat{J}^{C2}u) - (\hat{J}^C_+u)(\hat{J}^C{}_-u) + (\hat{J}^C_zu)^2] \qquad (9)$$

This constitutes an effective two-body model for which a Smoluchowski equation representing the rotational diffusion of two interacting rotors is solved.[15,16] The solution features three eigenvalues (correlation times) for the local motion when $S^2 = 0$:

$$(\tau_K)^{-1} = 6R^L_\perp + K^2(R^L_{||} - R^L_\perp) \text{ for } K = 0; 1; 2 \qquad (10)$$

Each K value leads to its own spectral density component.[21] Even for $S^2 > 0$ the $j_{K=1}(\omega)$ and $j_{K=2}(\omega)$ components are mainly dominated by local motions, whereas the $j_{K=0}(\omega)$ component represents mixed modes between the global and the local ($R^L_\perp$) motions. The "measurable" spectral density is then constructed out of the three $j_K(\omega)$ components by incorporation of the orientation-dependent functions that multiply the spin operators in the spin Hamiltonian.[21]

Assuming that the ^{15}N CSA tensor is axially symmetric and collinear with the dipolar N−H tensor ($\theta = 0$ in Figure 1b) the spectral density for ^{15}N CSA and ^{15}N−{^{1}H} dipolar relaxation in the coordinate frame of the local motion is given by:[14,21]

(21) Freed, H. J.; Nayeem, A.; Rananavare, S. B. *The Molecular Dynamics of Liquid Crystals*; Luckhurst, G. R., Veracini, C. A., Eds.; Kluwer Academic Publishers: The Netherlands, 1994; Chapter 12, pp 271−312.

$$J(\omega) = Aj_{K=0}(\omega) + Bj_{K=1}(\omega) + Cj_{K=2}(\omega) \qquad (11)$$

where $A = (1.5\cos^2\beta_{MD} - 0.5)^2$, $B = 3\sin^2\beta_{MD}\cos^2\beta_{MD}$, $C = 0.75\sin^4\beta_{MD}$, and β_{MD} is the "diffusion tilt" angle between the molecular diffusion axis Z_M and the N−H bond. In the present study the SRLS parameters featured by $J(\omega)$ include three diffusion rate constants, R^C, $R^L_\perp$, $R^L_{||}$, one potential parameter, c_{20}, and the polar angle β_{MD} (diffusion tilt) between the M and D frames (Figure 1). Special cases include the following: (1) isotropic fast local diffusion (local correlation time $\tau_f \equiv \tau_\perp = (6R^L_\perp)^{-1} \approx \tau_{||} = (6R^L_{||})^{-1}$), implying $\beta_{MD} = 0$; then, $J(\omega) = j_{K=0}(\omega)$, and the NMR relaxation data can be fit with one (c_{20}, if τ_f is negligibly small) or two (c_{20} and τ_f) free parameters, in complete analogy with the original model-free formulation;[4,5] (2) very anisotropic slow local motion ($\tau_f \equiv \tau_{||} \ll \tau_s \equiv \tau_\perp$ and $\tau_f \rightarrow 0$), denoted VALM below; then the last two terms in eq 11 are negligibly small compared to $Aj_{K=0}$, provided $\beta_{MD} \neq 54.7°$, and NMR data can be reproduced with three free parameters (c_{20}, τ_s, β_{MD}). The coefficient A in eq 11 is formally analogous to the squared order parameter S_f^2, while S_{SRLS}^2 (where S_{SRLS} is calculated using eq 3) is formally analogous to S_s^2, in the extended MF formula recast for $\tau_f \rightarrow 0$:[6]

$$J(\omega) = S_f^2[S_s^2\tau_m/(1 + \omega^2\tau_m^2) + (1 - S_s^2)\tau'_s/(1 + \omega^2\tau'^2_s)] \qquad (12)$$

where S_s and S_f are order parameters associated with the slow and fast local motions, respectively, τ_m is the correlation time of the global motion, and τ'_s is the effective correlation time of the slow local motion. Within the scope of VALM the fast local motion represents diffusion about an axis close to the N−H bond (Z_M in Figure 1b), and the slow local motion represents diffusion of the axis itself (about Y_M). A formal correspondence between the extended MF order parameter $S = S_fS_s$ and the SRLS order parameter, S_{SRLS}, can be established with the relation:

$$S \equiv S_{SRLS}(1.5\cos^2\beta_{MD} - 0.5) \qquad (13)$$

If NMR data at more than one magnetic field are available VALM can be extended to any degree of anisotropy in R^L by including an additional free parameter $\tau_f \equiv \tau_{||}$. Then all the $j_K(\omega)$ components contribute to $J(\omega)$ in eq 11. A formal analogy is thus established between the extended MF formula[6] and VALM.[22] The global correlation time τ_m is not considered a free parameter in the present context, where we focus on the microdynamic parameters; it should be determined independently.

In principle, the CSA and dipolar magnetic tensors are not collinear (Figure 1b). Then, in the local diffusion coordinate frame the dipolar and CSA spectral densities differ. The CSA spectral density can then be corrected for noncollinearity[23] with $\Delta J(\omega,\theta,\beta_{MD},\gamma_{MD})$ calculated by applying two consecutive rotations: from the M frame to the D frame and from the D frame to the CSA frame. In its most general form this correction term can be expressed as:

$$\Delta J(\omega) = 3/4\{[j_{K=0}(\omega) - j_{K=1}(\omega)]F_a - [j_{K=1}(\omega) - j_{K=2}(\omega)]F_b\} \qquad (14)$$

F_a and F_b are complex trigonometric functions of the angles θ, β_{MD}, and γ_{MD}.[23]

Numerical simulations showed that the sensitivity of ^{15}N T_1, T_2, and ^{15}N−{^{1}H} NOE to γ_{MD} increases with magnetic field strength because of the augmented CSA contribution. In general, the sensitivity of T_1 and T_2 to γ_{MD} variations is limited, while NOEs are approximately twice less sensitive to γ_{MD} than T_1 and T_2. To avoid an excess of free variables we fixed γ_{MD} at 90°. Then the perpendicular local motion represents excursions of the Z_M axis out of the peptide plane approximately about the $C^\alpha(i-1)-C^\alpha(i)$ axis (Figure 1b).

After the spectral density function $J(\omega)$ has been constructed out of its fundamental $j_K(\omega)$ components by using eq 11, the measurable ^{15}N relaxation quantities ^{15}N T_1, ^{15}N T_2, and ^{15}N−{^{1}H} NOEs are calculated as a function of $J(0)$, $J(\omega_N)$, $J(\omega_H)$, $J(\omega_H+\omega_N)$ and $J(\omega_H-\omega_N)$, using standard expressions for NMR spin relaxation.[3,24]

Methods and Calculations

The complete SRLS computational strategy, including the optimal choice of the basis set, was described previously.[15,16] The calculation of SRLS spectral densities is computationally intensive for c_{20} values exceeding ~10 (S^2 exceeding ~0.81) and/or very fast internal motions. Therefore, we used precalculated two-dimensional grids of $j(0)$, $j(\omega_N)$, $j(\omega_H)$, $j(\omega_H+\omega_N)$, and $j(\omega_H-\omega_N)$ to fit experimental ^{15}N T_1, T_2, and ^{15}N−{^{1}H} NOE data. The $j_{K=0}$, $j_{K=1}$, and $j_{K=2}$ grids of spectral density values at the five frequencies were constructed under the assumption of isotropic global motion for sets of c_{20} and τ_f (or τ_s) values. An axial ^{15}N chemical shielding tensor with $\tau_{||} - \tau_\perp = -170$ ppm, and $\theta = -16°$,[23] were used in these calculations. The c_{20} grid dimension spanned the values between 0 ($S^2 = 0$) and 40 ($S^2 = 0.95$), and the τ dimension spanned the values between $0.0005\tau_m$ and $1.4\tau_m$. A two-dimensional polynomial interpolation on the pre-constructed grid using Neville's algorithm[25] was employed for spectral density evaluation in the course of model fitting. The spectral density values at a fixed frequency are smooth functions of both c_{20} and τ, and can be reliably interpolated. The interpolation errors in both the c_{20} and τ grid dimensions were estimated to be at least 1 order of magnitude smaller than the errors in microdynamic parameters assessed with currently available experimental NMR techniques.

The fitting of experimental NMR data was based on target function minimization. For measurements carried out at one magnetic field the target function for spin i was defined as the sum of the squared differences between experimental and calculated T_1, T_2, and NOE values divided by the squared random errors:

$$\chi^2_i = [(T_{1i}^{obs} - T_{1i}^{calc})/\sigma_{T_1,i}]^2 + [(T_{2i}^{obs} - T_{2i}^{calc})/\sigma_{T_2,i}]^2 + [(NOE^{obs}_i - NOE^{calc}_i)/\sigma_{NOE,i}]^2 \qquad (15)$$

The SRLS-based dynamic models employed in the fitting procedure are summarized in Table 1. In model 1 the local motion is so fast ($\tau_f \rightarrow 0$) that its effect on the spectral density is negligible. This assumption is equivalent in practice to fixing τ at the lowest value for which the SRLS spectral densities could be calculated. In model 2 it is assumed that the internal motion can be approximated as isotropic ($\tau_\perp = \tau_{||}$). This model is analogous to the original MF formulation. Models 3 and 4 are derived from models 1 and 2, respectively, by addition of the free parameter R_{ex} to the transverse relaxation rate expressions, to account for possible exchange processes on the microsecond to millisecond time scale. For models 1−4, $\beta_{MD} = 0$, hence $J(\omega) = j_{K=0}(\omega)$ in eq 11 and the correction $\Delta J(\omega)$ in eq 14 depends solely on

(22) The term $(1 - S_f^2)\tau_f/(1 + \omega^2\tau_f^2)$, which should be added to eq 12 if no assumptions about τ_f are made, is formally analogous to the second term on the right-hand side of eq 11, as $S_f = (1.5\cos^2\beta_{MD} - 0.5)$ and $(1 - S_f^2) \approx 3\sin^2\beta_{MD}\cos^2\beta_{MD}$ for small β_{MD}. The third term of eq 11 can be neglected, as $\sin^4\beta_{MD}$ is very small in this case.

(23) Fushman, D.; Cowburn, D. *J. Biomol. NMR* **1999**, *13*, 139−153.

(24) Abragam, A. *Principles of Nuclear Magnetism*; Oxford University Press: Oxford, UK, 1960.

(25) Press, W. H.; Teukolsky, S. A.; Vetterling, W. T.; Flannery, B. P. *Numerical Recipes In C. The Art of Scientific Computing*; Cambridge University Press: Cambridge, UK, 1992.

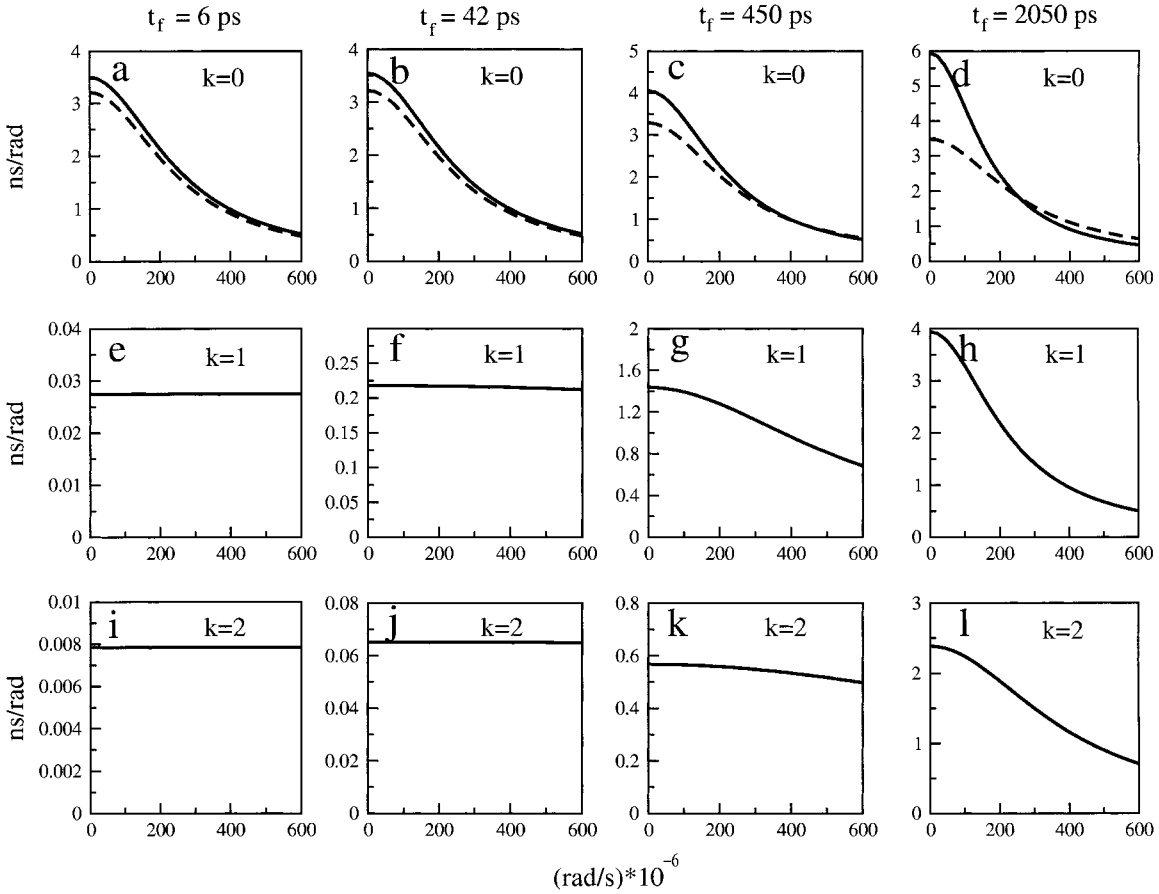

Figure 3. The low-frequency regions of SRLS $j_{K=0}(\omega)$, $j_{K=1}(\omega)$, and $j_{K=2}(\omega)$ (solid lines) and MF $J(\omega)$ (dashed lines) functions calculated for $\tau_m = 4.0$ ns for several values of the internal motion correlation time (τ_f). The internal motion was assumed to be isotropic.

Table 1. SRLS Models Used to Fit Experimental ^{15}N NMR Relaxation Data Acquired at One Magnetic Field

model no.	parameters[a]	SRLS model description
1	$c_{20}(S^2)$	very fast internal motion ($\tau \rightarrow 0$)[b]
2	$c_{20}(S^2)$; $\tau(\tau_f)$	isotropic internal motion
3	$c_{20}(S^2)$; R_{ex}	model 1 with exchange term
4	$c_{20}(S^2)$; $\tau(\tau_f)$; R_{ex}	model 2 with exchange term
5	$c_{20}(S_s^2)$; $\beta_{MD}(S_f^2)$; $\tau_\perp(\tau_s)$	very anisotropic slow local motion[c]

[a] Analogous MF parameters are shown in parentheses. [b] For model 1 the $\tau \rightarrow 0$ assumption is practically equivalent to fixing τ at the lowest value for which the SRLS spectral densities can be calculated. [c] For model 5 it is assumed that $\tau_{||} \rightarrow 0$. This assumption is equivalent to neglecting the $j_{K=1}(\omega)$ and $j_{K=2}(\omega)$ spectral density components.

the angle θ. In model 5 the local motion is anisotropic. To be able to fit the data acquired at one magnetic field (3 observables) model VALM ($\tau_f \equiv \tau_{||} \ll \tau_s \equiv \tau_\perp$, and $\tau_f \rightarrow 0$) was used. In this case only $\tau_\perp$ (or $j_{K=0}(\omega)$) enters the spectral density. The angle β_{MD} was allowed to vary. The VALM form of $J(\omega)$ is analogous to the extended MF formula[6] with τ_f set equal to 0.

The model selection scheme based on χ^2- and F-testing closely followed that of the widely used MF procedure.[26] Briefly, if model 1 did not pass the χ^2-test with 10% confidence level, the χ^2- and F-statistic testing were performed for the two-parameter models 2 and 3 versus model 1. If these latter tests were not successful, the Q probability level was lowered (typically to 0.1%) and the tests were performed anew for models 1−3. The three-parameter models 4 and 5 were used only if all the previous tests failed. Since the number of parameters in models 4 and 5 is equal to the number of NMR observables at one field, neither χ^2- nor F-testing were possible. The residual χ^2 values for models 4 and 5 was required to be lower than 10^{-5}. The described model fitting and model-selection schemes were implemented in a fitting program used for SRLS data analysis. Error estimation of the fitted parameters was carried out using 100 Monte Carlo simulations.[27]

The 2D grids were generated on a Microway workstation equipped with a 500 MHz Digital Alpha 21264 processor and a 500 MB memory. The CPU time required was 10 days for the $j_{K=0}(\omega)$ grid, and 20 days for each of the $j_{K=1}(\omega)$ and $j_{K=2}(\omega)$ grids, with several c_{20} values exceeding 20. Once the grids were generated, they could be rapidly and repeatedly utilized in fitting experimental data.

Results and Discussion

The low-frequency regions of all three K components of $J(\omega)$, calculated for isotropic global motion with $\tau_m = 4$ ns, are shown in Figure 3 as a function of the time scale separation between the local and global motions. The $j_{K=1}(\omega)$ and $j_{K=2}(\omega)$ components (Figure 3e−h,i−l) are dominated by the local motion and are almost independent of c_{20}. They contribute significantly to the "measurable" $J(\omega)$ only for slow local motions. The $j_{K=0}(\omega)$ component is similar to the MF spectral density (Figure 3a−d). In general, model-free underestimates spectral density values at low frequencies and slightly overestimates them at higher ones. These differences become more significant for higher values of c_{20} (not shown) and slower local motions, i.e. with decreasing time scale separation between the local motion and the overall tumbling (cf. Figure 3a−d). It is important to note that for low ordering MF was shown to represent a limiting case of the SRLS theory.[15] It was also shown that a small SRLS coupling potential has the same effect as anisotropic local diffusion,[13] which manifests as an increase in $j_{K=0}(0)$ as compared to isotropic local diffusion. It can be shown that SRLS

(26) Mandel, A. M.; Akke, M.; Palmer, A. G., III *J. Mol. Biol.* **1995**, *246*, 144−163.

(27) Kamath, U.; Shriver, J. W. *J. Biol. Chem.* **1989**, *264*, 5586−5592.

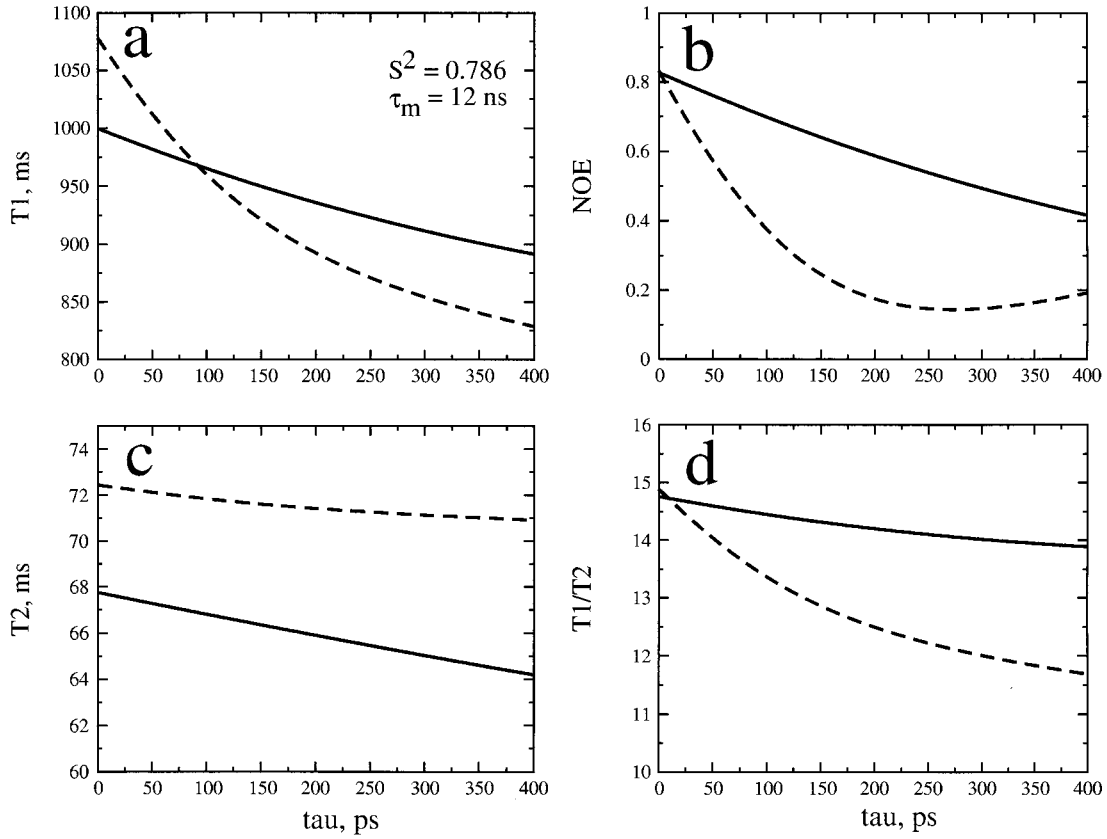

Figure 4. Theoretical curves of (a) ^{15}N T_1 (ms), (b) ^{15}N−{^{1}H} NOE, (c) ^{15}N T_2 (ms), and (d) the T_1/T_2 ratio as a function of the local motion correlation time τ_f (ps) for SRLS (solid lines) and MF (dashed lines) calculated for $S^2 = 0.786$, $\tau_m = 12.0$ ns, and 14.1 T magnetic field.

also converges to MF in the limit of very high ordering ($S^2 \rightarrow 1$) and very fast local motions ($\tau_f \equiv (6R_{||}^L)^{-1} \rightarrow 0$). In this limit the SRLS $j_{K=0}(\omega)$ component approaches asymptotically the MF spectral density, i.e. a Lorentzian $\tau_m/[1 + (\omega\tau_m)^2]$ representing global motion. Numerical simulations carried out for $\tau_m = 4$ ns and $\tau_f = 2$ ps, i.e., a time scale separation of 0.0005, showed that the contribution of the global motion ($S^2\tau_m$) constitutes over 99.98% of $J(0)_{(MF)}$ for $0.75 \leq S^2 \leq 0.95$. Although the pure global motion dominates $J(0)_{(SRLS)}$, there are also additional contributions due to mixed modes. The relative difference $\Delta J(0) = [J(0)_{SRLS} - J(0)_{MF}]/J(0)_{SRLS}$ was found to range from 9% for $S^2_{SRLS} = 0.75$ to 5% for $S^2_{SRLS} = 0.95$. Since with currently available NMR techniques the typical experimental error in T_2, which in this limit constitutes a very good approximation to the error in $J(0)$, is below 2%, we conclude that in the range of order parameters relevant for folded proteins ($c_{20} = 4 \div 40$) ^{15}N relaxation data are sensitive to the presence of mixed modes even when the local motion is in the extreme narrowing limit.

Theoretical ^{15}N T_1, T_2, ^{15}N−{^{1}H} NOE, and T_1/T_2 curves, calculated as a function of τ_f with both SRLS and MF for $S^2 = 0.786$, $\tau_m = 12$ ns, and 14.1 T, are shown in Figure 4. It can be seen that the SRLS-derived T_1 and NOE values change as a function of the local motion to a much larger extent than the MF-derived values (Figure 4a,b), while the T_2 values change comparably (Figure 4c). In the $\tau_f \rightarrow 0$ limit the T_1/T_2 ratio (Figure 4d) predicted by both theories is approximately the same. Therefore, the determination of τ_m based on T_1/T_2 ratios of "rigid" ($\tau_f \rightarrow 0$) spins[28] should give similar results. SRLS predicts the T_1/T_2 analysis to be more robust because SRLS T_1/T_2 ratios are less sensitive to local motions than their MF counterparts. A better alternative for τ_m determination, pursued in this study using SRLS, is based on searching for the minimum value of the sum of χ^2 residuals for all the protein residues and a maximum sum of degrees of freedom (df). In practice, we looked for a minimum in the sum of χ^2/df over all the protein residues. Both approaches resulted in τ_m values very similar to those derived using MF.

Numerical simulations were carried out using SRLS-derived synthetic ^{15}N T_1, T_2, and NOE data sets with subsequent parametric fitting using MF. Figure 5a illustrates relative errors in the derived order parameters ($[S^2_{MF} - S^2_{SRLS}]/S^2_{SRLS}$) for spins with negligible local motions. In this regime the extent of S^2 overestimation by MF was found to be weekly field dependent in the range of 11.7−18.7 T and almost independent of the global correlation time. The τ_m values calculated from T_1/T_2 ratios[28] using MF were essentially the same as those obtained using SRLS. The correlation times for fast internal motions were underestimated by MF more than 2-fold (Figure 5b). For models with slow (very anisotropic) internal motions the relative differences in the obtained order parameters are approximately twice higher (cf. Figure 5c,d). For a fixed local motion correlation time these differences are strongly dependent on τ_m, which in this case determines the time scale separation between the two modes (Figure 5c). The smaller the time scale separation between the global and local motions, the higher is the extent to which S^2 is overestimated by MF. The time scale separation between the local and the global motions also controls the relative differences in the slow motion correlation times (Figure 5d). These results indicate that in the parameter range relevant for folded proteins the order parameters are significantly overestimated, whereas local motion correlation times are considerably underestimated by MF.

(28) Kay, L. E.; Torchia, D. A.; Bax, A. *Biochemistry* **1989**, *28*, 8972−8979.

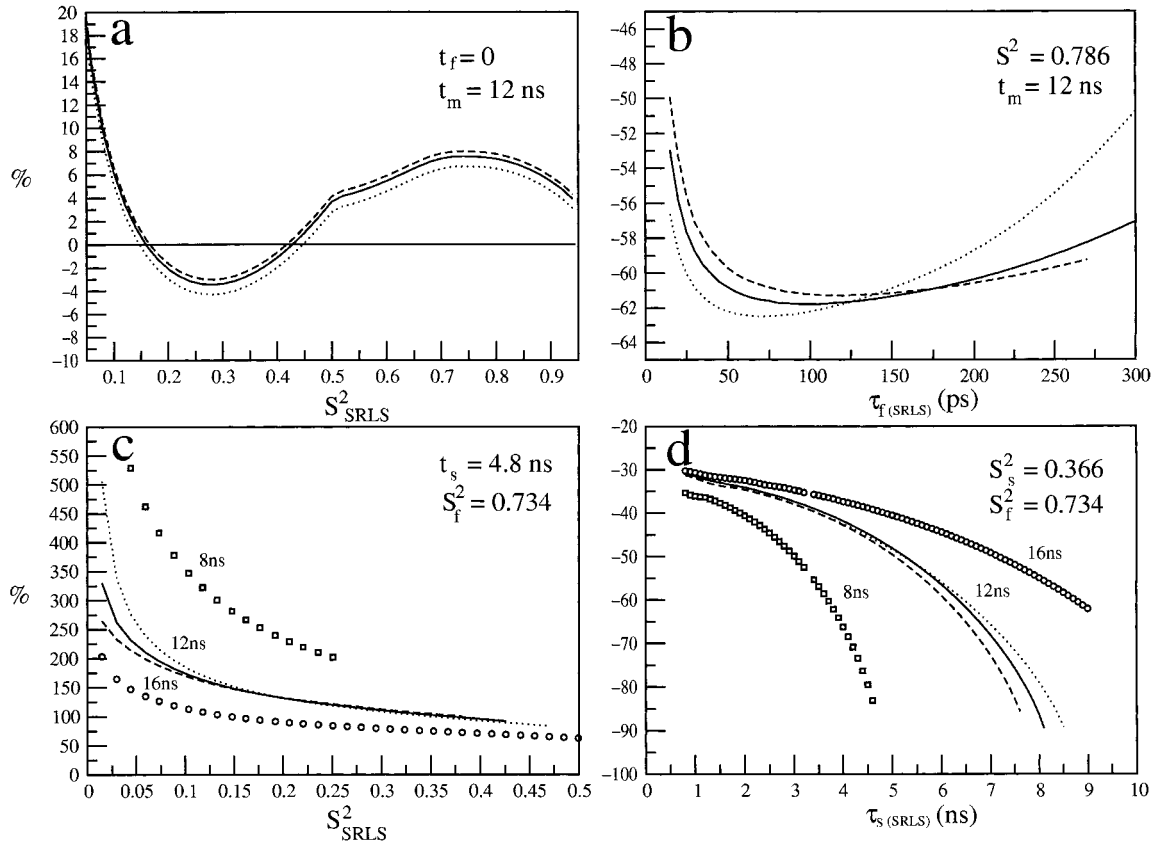

Figure 5. Relative errors of SRLS and MF parameters associated with numerical simulations using the synthetic SRLS data fit with MF, shown as percent deviations: (a) $[S^2_{(MF)} - S^2_{(SRLS)}]/S^2_{(SRLS)}$ versus $S^2_{(SRLS)}$ for magnetic fields of 11.7 (dotted line), 14.1 (solid line), and 18.7 T (dashed line) for $\tau_f = 0$ and $\tau_m = 12$ ns. (b) $[\tau_{f(MF)} - \tau_{f(SRLS)}]/\tau_{f(SRLS)}$ versus $\tau_{f(SRLS)}$ for magnetic fields as denoted in panel a, for $S^2_{(SRLS)} = 0.786$ and $\tau_m = 12$ ns. (c) $[S^2_{(MF)} - S^2_{(SRLS)}]/S^2_{(SRLS)}$) versus $S^2_{(SRLS)}$ for $\tau_s = 4.8$ ns and $S^2_f = 0.734$. Data are given for $\tau_m = 8$ (squares), 12 , and 16 ns (circles). For $\tau_m = 12$ ns the field dependence is also shown, as denoted in panel a. (d) $[\tau_{s(MF)} - \tau_{s(SRLS)}]/\tau_{s(SRLS)}$ versus $\tau_{s(SRLS)}$ for $S^2_s = 0.366$ and $S^2_f = 0.734$. Data are given for $\tau_m = 8$ (squares), 12, and 16 ns (circles). For $\tau_m = 12$ ns the field dependence is also shown, as denoted in panel a.

The SRLS-based analysis was tested extensively on ^{15}N relaxation data from several isotropically tumbling proteins. RNase H from *E. coli*, extensively studied previously with MF,[26,29] is chosen here as an illustrative example of the results of the SRLS-based fitting. The anisotropy of the global tumbling of RNase H was shown[29] to be low ($\tau^m_\perp/\tau^m_\parallel = 1.12$). A global effective correlation time of $\tau_m = 9.28$ ns was used to calculate microdynamic parameters both in the previous MF studies[29] and in our SRLS analyses. Out of 124 spins, 121 could be fit using SRLS spectral densities. For 109 spins analogous models were selected by both methods. The details of the SRLS-based fitting are provided in the Supporting Information (Table 1S). Figure 6 shows the superposition of the SRLS- and model-free-derived microdynamic parameters for those residues where analogous models, i.e., models with the same number of corresponding parameters, were selected. While for models with local motions on the picosecond time scale the average reduction in S^2 is in the range of 7−9%, for models with nanosecond local motions S^2 can be two-to-three times lower than the corresponding SRLS value (Figure 6a). The local motion correlation times on both the picosecond (Figure 6b) and nanosecond (Figure 6c) time scales are typically underestimated by MF by at least a factor of 2. Both treatments yield practically identical exchange contributions (Figure 6d). This indicates that for the R_{ex}-featuring models the exchange term does not absorb the differences between SRLS and MF microdynamic parameters. The effect of γ_{MD} on the results was checked by fitting the data with $\gamma_{MD} = 0°$ and 180°. The patterns illustrated in Figure 6 were found to be preserved, in accordance with the relatively small effect of γ_{MD} variability on the NMR observables at 11.7 T. Interestingly, the very study providing the experimental RNase data[29] used herein focuses on the quantitative relation between the magnitude of S^2 and conformational entropy contributions. In this context the accuracy of S^2 is of considerable importance. It is also of interest to note that in general underestimation of correlation times for local motion may impact the determination of τ_m based on T_1/T_2 considerations.[28]

The fundamental feature that singles out SRLS with respect to MF is the inclusion of mixed modes in the former and their omission in the latter. It is quite intriguing that even when the internal motion is in the extreme motional narrowing limit, the experimental NMR data are sensitive enough to bear out the contribution of mixed modes in the typical range of high ordering experienced by N−H bond vectors in proteins.

If NMR relaxation data acquired at more than one magnetic field are available, both angles β_{MD} and γ_{MD} can be determined in principle. These angles fix the orientation of the local diffusion and local ordering axes, while their magnitude is determined by the local surroundings of the N−H bond vector. Thus, local structure affects local geometry via dynamical coupling. Domain motions of the kind encountered in many enzymes[30−32] exemplify more indirect elements of dynamic structure, where mode-coupling is expected to have important implications. In such cases SRLS is expected to help correlate structural dynamics with function.

(29) Mandel, A. M.; Akke, M.; Palmer, A. G., III *Biochemistry* **1996**, *35*, 16009−16023.

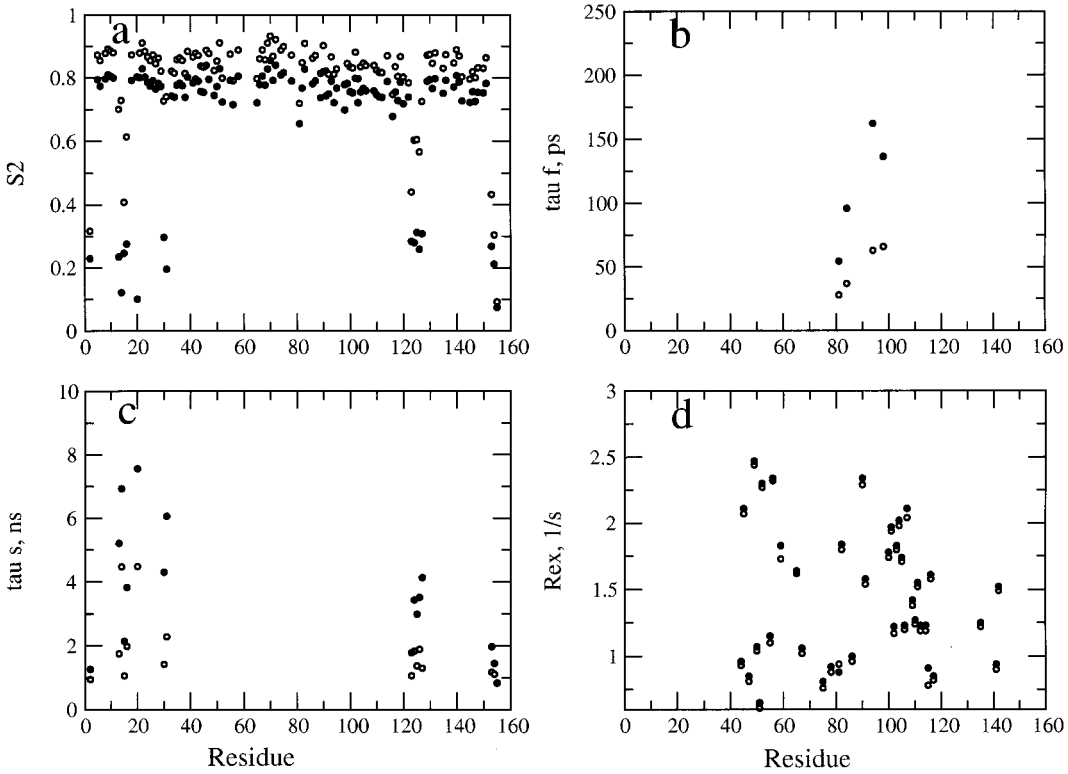

Figure 6. Best fit microdynamic parameters of *E. coli* RNase H, based on data acquired at 300 K and 11.7 T, obtained using SRLS (solid circles) and MF (opaque circles) spectral densities: (a) squared order parameters; (b) fast local motion correlation times; (c) slow local motion correlation times; and (d) exchange contributions. The MF data were taken from the literature.[29] For SRLS model 5 the order parameter is calculated as the product of S_{SRLS}^2 and $(1.5\cos^2\beta_{MD} - 0.5)^2$, where S_{SRLS} is equivalent to S_s and $(1.5\cos^2\beta_{MD} - 0.5)$ to S_f in the extended MF formulas.

The $j_{K=1}(\omega)$ and $j_{K=2}(\omega)$ spectral density contributions are associated with axial local diffusion and ordering tensors and nonzero "diffusion tilt" angles (β_{MD}). Models with $\beta_{MD} \neq 0$ (VALM) are therefore indicative of the fact that MF effective correlation times and generalized order parameters are no longer adequate descriptors of internal motions and local ordering. Rather, tensorial properties must be assigned to these variables. We found that experimental ^{15}N NMR relaxation data featuring slow motions cannot be reproduced with eq 11 using the assumption of isotropic local diffusion. This is actually the consequence of the relatively high axial local ordering and small time scale separation between τ_m and τ_s.

It is of interest to pinpoint the basic tenets of the mode-coupling diffusion theory[7−9] and the GAF model[10−12] in the SRLS context. The mode-coupling diffusion theory as applied to ^{15}N relaxation in proteins could not account for data acquired above 8.4 T, apparently because it focuses on the weight of the global diffusion mode, but precludes the manifestation of mixed modes in the correlation function. It should be noted that currently this approach is limited to very fast local motions because of practical restraints imposed by the length of the molecular dynamics simulations. The 3D GAF model reinterprets S^2 in terms of restricted fast fluctuations about three orthogonal axes.[11] When applied to ^{15}N relaxation data it only treated spins with internal motions below 50 ps.[12] The manifestation of mixed modes is precluded because decoupling between global and internal motions is assumed.[33] Hence, both approaches apply to the extreme narrowing limit without properly accounting for mixed modes.

SRLS is also applicable to cross-correlated relaxation studies.[36] There are quite a few literature reports where MF enhanced by GAF could not interpret ^{13}C-related cross-correlated relaxation rates,[37] which for larger proteins depend primarily on $J(0)$. As shown in Figure 3a−d, even when $\beta_{MD} = 0$ the MF and SRLS spectral densities at $\omega = 0$ differ significantly. Interestingly, Lee and Wand[38] assigned problems with the interpretation of multifrequency autocorrelated ^{15}N relaxation data of Ubiquitin to MF deficiencies in properly predicting $J(0)$.

In summary, the theoretical treatment of ^{15}N protein relaxation data is extended in this study to account for dynamical coupling between global and local motions. The tensorial properties of the two-body SRLS model provide ample opportunities for a physically meaningful interpretation of NMR relaxation data in proteins. It can be applied to other NMR heteronuclei[37,39]

(30) (a) Hayward, S. *Proteins: Struct. Funct. Genet.* **1999**, *36*, 425−435. (b) Yan, H. *Advances in Enzymology and Related Areas of Molecular Biology*; Purish, D. L., Ed.; John Wiley & Sons: New York, 1999; Vol. 73.

(31) (a) Sinev, M. A.; Sineva, E. V.; Ittah, V.; Haas, E. *Biochemistry* **1996**, *35*, 6425−6437. (b) Sinev, M. A.; Sineva, E. V.; Ittah, V.; Haas, E. *FEBS Lett.* **1996**, *397*, 273−276.

(32) Shapiro, Y. E.; Sinev, M. A.; Sineva, E. V.; Tugarinov, V.; Meirovitch, E. *Biochemistry* **2000**, *39*, 6634−6644.

(33) Very recently Bruschweiler and co-workers have employed a procedure of analyzing computed molecular dynamics trajectories in terms of quasiharmonic modes to extract a description of intramolecular protein dynamics, and related it to nuclear spin relaxation.[34,35] This is entirely different from our approach since we fit the experimental nuclear spin relaxation data from each local site of the protein to an appropriate stochastic model, viz. the SRLS model. It would be of relevance, in the future, to relate the results of our method of analysis of nuclear spin relaxation data to molecular dynamics, and Bruschweiler's procedure for analyzing the latter could prove useful in this regard.

(34) Lienin, S. F.; Brüschweiler, R. *Phys. Rev. Lett.* **2000**, *84*, 5439−5442.

(35) Prompers, J. J.; Brüschweiler, R. *J. Phys. Chem. B* **2000**, *104*, 11416−11424.

(36) Tjandra, N.; Szabo, A.; Bax, A. *J. Am. Chem. Soc.* **1996**, *118*, 6986−6991.

(37) Carlomagno, T.; Maurer, M.; Hennig, M.; Griesinger, C. *J. Am. Chem. Soc.* **2000**, *120*, 5105−5113.

(38) Lee, A. L.; Wand, J. *J. Biomol. NMR* **1999**, *13*, 101−112.

and anisotropic global tumbling. It is expected that exploring the option of complete anisotropic ordering for high order parameters and fast local motions will also become feasible.

Acknowledgment. This work was supported by the Israel Science Foundation grant No. 520/99-16.1 to E.M. and the NIH grant No. RR07126 to J.H.F. E.M. gratefully acknowledges the hospitality of CSIT, FSU, Tallahassee, FL, during short visits promoting this work; we also thank CSIT for computational resources. We thank Dr. David Fushman (University of Maryland, MD) for sharing with us his program DYNAMICS.

Supporting Information Available: Table 1S giving the results of SRLS fitting of *E. coli* RNase H ^{15}N relaxation data including estimated errors of the best-fit parameters (PDF). This material is available free of charge via the Internet at http://pubs.acs.org.

JA003803V

(39) Yang, D. W.; Mittermaier, A.; Mok, Y. K.; Kay, L. E. *J. Mol. Biol.* **1998**, *276*, 939−954.